

A New Capture Fraction Method to Map How Pumpage Affects Surface Water Flow

by Stanley A. Leake¹, Howard W. Reeves², and Jesse E. Dickinson³

Abstract

All groundwater pumped is balanced by removal of water somewhere, initially from storage in the aquifer and later from capture in the form of increase in recharge and decrease in discharge. Capture that results in a loss of water in streams, rivers, and wetlands now is a concern in many parts of the United States. Hydrologists commonly use analytical and numerical approaches to study temporal variations in sources of water to wells for select points of interest. Much can be learned about coupled surface/groundwater systems, however, by looking at the spatial distribution of theoretical capture for select times of interest. Development of maps of capture requires (1) a reasonably well-constructed transient or steady state model of an aquifer with head-dependent flow boundaries representing surface water features or evapotranspiration and (2) an automated procedure to run the model repeatedly and extract results, each time with a well in a different location. This paper presents new methods for simulating and mapping capture using three-dimensional groundwater flow models and presents examples from Arizona, Oregon, and Michigan.

Introduction

“Capture” is withdrawal-induced changes in inflow to or outflow from an aquifer. The concept was first clearly articulated by Theis (1940). He explained that the source of water derived by wells as initially from storage and later can be from increased inflow to and decreased outflow from the aquifer. Bredehoeft et al. (1982) further explained concepts of capture and emphasized that development of water resources should depend on the amount of water that can be captured with acceptable consequences, not on the amount of recharge an aquifer receives. Capture that results in a loss of water in streams, rivers, and wetlands is of concern in many parts of the United States because of degradation

of groundwater-dependent ecosystems and reduction of surface water supplies for which there are existing water rights.

Glover and Balmer (1954) developed an analytical solution to compute time-dependent capture of water in a river by an adjacent well withdrawing groundwater at a constant rate. Although this and related analytical solutions are still in use, numerical models such as MODFLOW (Harbaugh et al. 2000) allow more flexibility in consideration of complex aquifer and surface water geometries and heterogeneous aquifer properties. The most common applications of numerical models are to calculate capture vs. time at a few specific locations, such as existing or proposed well locations. For examples of these applications, see Bredehoeft et al. (1982), Gannett and Lite (2004), and Leake et al. (2005). In the example by Bredehoeft et al. (1982), a hypothetical aquifer system is used to show the timing of capture with two different locations of a well field consisting of many wells.

Capture can be expressed as an instantaneous flow rate of depletion of surface water or evapotranspiration at a given time or as the total volume of depletion since pumping began. In this work, it is proposed that expressing capture as a dimensionless fraction of change

¹Corresponding author: U.S. Geological Survey, 520 N. Park Ave., Suite 221, Tucson, AZ 85719; 520-670-6671 ext. 259; fax: 520-670-5592; saleake@usgs.gov

²U.S. Geological Survey, Lansing, MI 48911.

³U.S. Geological Survey, Tucson, AZ 85719.

Received December 2008, accepted March 2010.

Journal compilation © 2010 National Ground Water Association.

No claim to original US government works.

doi: 10.1111/j.1745-6584.2010.00701.x

in flow divided by the withdrawal rate that causes the change in flow is most useful in understanding the expected depletion rates by pumping for any given time. Moreover, use of the dimensionless fractions in relation to pumping rate can be used to determine ultimate or steady state capture from select features of interest (such as stream reaches, springs, etc.) resulting from pumping at a particular location. If a system responds linearly to groundwater withdrawals, that fraction is independent of the withdrawal rate. For example, if the capture fraction were 0.5 for a time and location of interest, the capture rate for a pumping rate of 100 m³/d would be 50 m³/d, and the capture rate for a withdrawal rate of 500 m³/d would be 250 m³/d. Similarly, that same capture fraction could be used to compute changes in inflow to or outflow from the aquifer in response to injection of water.

Capture fractions formulated as the ratio of capture rate to pumping rate also are a type of aquifer response function that is used in management optimization models of stream-aquifer systems (Maddock and Lacher 1991; Barlow and Dickerman 2001; Cosgrove and Johnson 2004). Most applications of these types of response functions in management optimization models involve computation of response functions at select locations of pumping wells. In contrast, this work focuses on computation and display of response functions (capture fractions) over large regions to help in understanding effects of pumping location on timing of capture or locations of features from which capture may occur, within a large set of possible pumping locations in an aquifer.

Several investigators have used analytical methods or numerical models to map the effects of pumping locations on surface water resources. Jenkins and Taylor (1974) presented a map of part of the Arkansas River Valley in Colorado showing lines of equal stream depletion factor (sdf), in days. That value is the time at which accumulated change in streamflow volume equals 28% of the volume pumped by a well pumping at a constant rate. In an ideal homogeneous semi-infinite aquifer with a straight fully penetrating stream, sdf can be computed as:

$$\text{sdf} = a^2 S / T, \quad (1)$$

where a is the distance from the pumping location to the stream, S is aquifer storage coefficient (specific yield), and T is transmissivity. Burns (1983) mapped areas of selected sdf values near the Platte River in southcentral Nebraska. More recently, the Platte River Cooperative Hydrology Study (COHYST Technical Committee 2004) used a numerical model to map the line of 28% volume depletion at a pumping time of 40 years for an area around the North Platte River in Nebraska. Regulation of the coupled groundwater-surface water system in that area dictates that capture or depletion be computed as a fraction of pumped volume since pumping begins. Peterson et al. (2008) used a numerical model to show ranges of base flow depletion as a percentage of volume pumped at 50 years for the Elkhorn and Loup River Basins, Nebraska.

An earlier version of the capture fraction calculation and mapping was presented by Leake et al. (2008b). They used a flow model of the Upper San Pedro Basin in southeastern Arizona, USA, and northern Sonora, Mexico, to display the fraction of pumping rate that is capture as a function of pumping location for several times of interest. Leake et al. (2008a) used simpler superposition models to map potential depletion of the Colorado River by pumping wells. Cosgrove and Johnson (2005) used the MODRSP code (Maddock and Lacher 1991) to compute maps of unit steady state response functions of river seepage to pumping for various reaches of the Snake River in Idaho. The unit response functions are the same as steady state capture fractions for a single feature described later in this paper. Here, transient capture fractions also are considered.

This work first describes the methods used to calculate capture fractions and difficulties related to model nonlinearity, execution time, and mass balance errors. The methods are then demonstrated using results from three field studies and one synthetic test case. The results and the utility and limitations of the method they demonstrate are discussed. Finally, conclusions about the new method are presented.

Methods

To compute capture using a groundwater flow model, the first step is to make a simulation without the added withdrawal to establish baseline values of all water budget components. The second step is to re-run the simulation with no other changes except for the added withdrawal. The third step is to compute changes in water budget components from the base case for select simulation times. The resulting capture curves serve a specific purpose but do not give aquifer managers a broader picture of how location and timing of withdrawals result in capture. To help fill this need, this paper presents methods for calculation of capture over large areas or volumes of an aquifer, for specific times of interest.

Examples presented in this paper use MODFLOW-88 (McDonald and Harbaugh 1988) and MODFLOW-2000 (Harbaugh et al. 2000; Hill et al. 2000) as the simulator for groundwater flow. However, the methods are generally applicable and would be useful for any groundwater flow model.

Constructing Capture Maps

In any groundwater model, a simulated pumping well can capture water from features represented by constant- or specified-head (Dirichlet), or head-dependent (Cauchy) boundary conditions, Neumann boundary conditions, which add or remove water at a specified flux or flow rate, do not enter into this analysis because new withdrawals do not change the flow to or from Neumann-type boundaries. The boundaries of concern in this work are those to which flow between the feature and aquifer is potentially affected by pumpage, or equivalently, the flow is subject to capture. Here, they are called features

subject to capture, or just features. Features subject to capture can be represented by an individual element, cell, or other elementary model component, or a group of components. They can represent rivers, streams, springs, lakes, and so on.

If a well at a given location withdraws water at rate, Q_{well} , then at time t the capture from n features will be $\Delta Q_{1,t} + \Delta Q_{2,t} + \dots + \Delta Q_{n,t}$. An individual capture value, $\Delta Q_{k,t}$, is defined as the difference between the rate of flow to or from feature k without the well withdrawing water, $Q_{k,t}$, and the rate of flow to or from the feature in an identical simulation with the withdrawal of water by the well, $Q'_{k,t}$.

Besides capture, the other source of water to a pumped well is change in storage in the aquifer. The change in the rate of water going into or out of storage at time t , $\Delta Q_{S,t}$ is defined as the difference between the rate of flow into or out of storage without the withdrawal of water, $Q_{S,t}$, and the rate of flow into or out of storage in an identical simulation with the withdrawal of water by the well, $Q'_{S,t}$. Quantities Q_{well} , $Q'_{k,t}$, $Q_{k,t}$, $Q_{S,t}$, and $Q'_{S,t}$ are volumetric flow rates [L^3/T]. Here, the sign convention is that negative values represent withdrawal or flow out of the groundwater system or into storage.

A general expression for mass balance accounting for the withdrawal Q_{well} at time t is:

$$Q_{\text{well}} = \Delta Q_{S,t} + \sum_{i=1}^n \Delta Q_{i,t}, \quad (2)$$

where n is the number of features from which capture can occur. In this equation, $\Delta Q_{S,t}$ is the difference in total storage change over the entire model grid. The summation, $\sum_{i=1}^n \Delta Q_{i,t}$, represents the total decrease in outflow to and (or) increase in inflow from all head-dependent flow boundaries in the system, or total capture. Dividing by Q_{well} , Equation 2 can be rewritten as:

$$1.0 = \Delta Q_{S,t}/Q_{\text{well}} + \sum_{i=1}^n \Delta Q_{i,t}/Q_{\text{well}}. \quad (3)$$

If a system responds linearly enough to withdrawals, the capture from a particular withdrawal rate Q_{well} can

be scaled proportionally to compute capture from another withdrawal rate, $a \times Q_{\text{well}}$, where a is a multiplicative factor. Issues related to nonlinearity are discussed after the types of capture maps are defined.

The capture maps considered in this work are produced using the following basic steps:

1. Run the model without the added withdrawal, Q_{well} , and save values of $Q_{1,t}$, $Q_{2,t}$, ..., $Q_{n,t}$, and $Q_{S,t}$. Here, n is the number of features being considered. It could be one or a potentially large number, up to the number of features included in the model.
2. For the region to be mapped, run a steady state or transient model with pumpage added at one location.
3. For steady state or at time t , compute $\Delta Q_{1,t}$, $\Delta Q_{2,t}$, ..., $\Delta Q_{n,t}$, and $\Delta Q_{S,t}$ using computed values of $Q'_{1,t}$, $Q'_{2,t}$, ..., $Q'_{n,t}$, and $Q'_{S,t}$, and saved values of $Q_{1,t}$, $Q_{2,t}$, ..., $Q_{n,t}$, and $Q_{S,t}$ from step 1.
4. Compute and save the total capture value, $\sum_{i=1}^n \Delta Q_{i,t}/Q_{\text{well}}$, the storage change value, $\Delta Q_{S,t}/Q_{\text{well}}$, and the x and y location of the well.
5. If simulations for all locations in the region to be mapped have been run, proceed to step 6. Otherwise, select a new location for pumpage and go back to step 2. For mapping capture, it may not be necessary to simulate pumpage at all grid locations. The runs involved are independent and fully parallelizable.
6. Use a GIS or other program to make a contour map of $\sum_{i=1}^n \Delta Q_{i,t}/Q_{\text{well}}$ for all of n features, or $\Delta Q_{k,t}/Q_{\text{well}}$ for a particular feature k .

For the three kinds of maps considered in this work, Table 1 shows choices made in the basic procedure.

For efficiency, steps 2 to 5 should be automated with a computer program that runs the model repeatedly, each time incrementing the well location, computing capture values and saving results. Information for computing capture from all features can be obtained from model mass balance calculations. Information needed to compute capture for individual features can be obtained from separate model output of flows to and from boundaries.

Basic information needed for making a map of transient capture is shown in Figure 1A, in which capture

Table 1
Choices in the Basic Procedure Needed to Produce the Three Types of Capture Maps Considered Here

Step	Type of Capture Map		
	Transient Capture from All Features	Transient Capture from One Feature	Ultimate Steady State Capture from One Feature
1 and 3—features to include	All features	One feature	One feature
2—transient or steady state	Transient	Transient	Steady state
6—results to be mapped	Map results for capture from all features	Map results for capture from one feature	Map results for capture from one feature

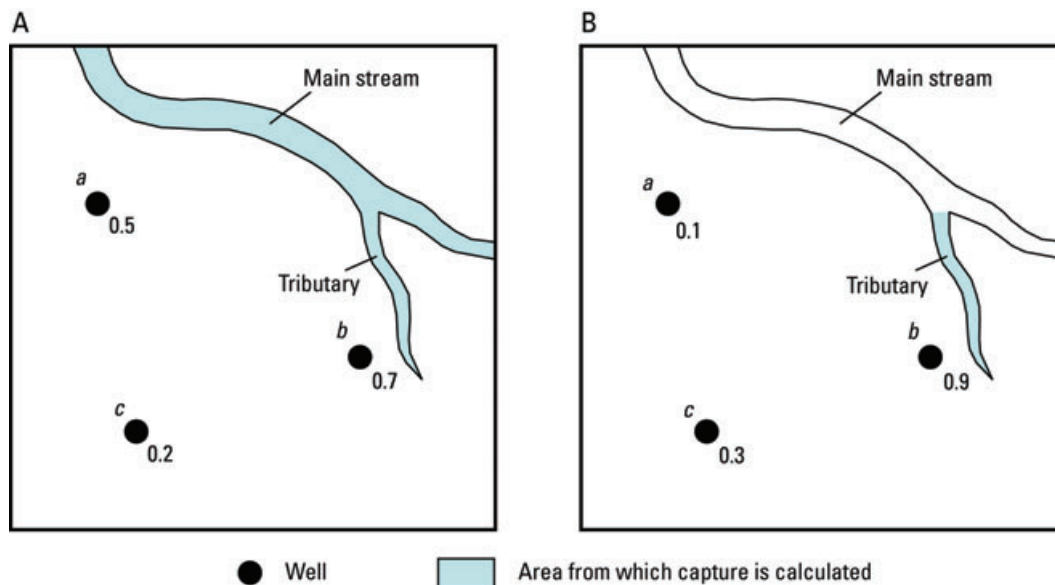


Figure 1. Schematic diagram showing computed capture for groundwater pumping at locations *a*, *b*, and *c*. Values in A are transient capture fractions that might occur from the main stream and the tributary at a specified time. Values in B are ultimate or steady state capture fractions from the tributary only.

for a time of interest has been calculated for pumping locations *a*, *b*, and *c*. The feature potentially subject to capture is the main stream and a tributary. The same pumping rate, Q_{well} , is imposed at first one point, then the other, then the other. At the specified time, the fractions of the pumping rate captured from the stream and tributary are 0.5, 0.7, and 0.2 at locations *a*, *b*, and *c*, respectively. Differences in capture values for these three points at the time of interest are influenced by their proximity to the main stream and tributary and the distribution of aquifer properties. To make a map of transient capture, these values and values for other locations would be contoured. In practice, the maximum density of points equals the number of grid cells, mesh nodes, and so on. Values in Figure 1B represent ultimate or steady state capture from one feature only, in this case the tributary to the main stream. Capture from the tributary at location *a*, 0.1, is the lowest because most of the capture there would be from the much closer main stream. In contrast, capture at point *b*, 0.9, is much higher because it is adjacent to the tributary. Capture at the more distant point *c*, 0.3, is intermediate. If the tributary and the main stream are the only boundaries or features from which capture can occur, then the ultimate capture fractions from the main stream only in this example would be 0.9, 0.1, and 0.7, respectively, for pumping locations *a*, *b*, and *c*. A map of steady state capture from the tributary could be made contouring these and capture values from other pumping locations.

Regardless of the type of map (Table 1) to be created, some preliminary work must be carried out before undertaking the steps described in the following sections. These include:

1. Select a region in the model over which to construct a capture map and the grid locations in that region for making capture calculations.
2. Select a constant well pumping rate for the capture calculations.
3. Determine how to compute change in boundary flow in the model from the added well.
4. Determine the simulation times at which to map capture (for transient analyses).

The preliminary steps are best carried out by running the model several times, with an added well at a different select location each time. Capture can be computed manually and results for these locations can help in selecting the final setup for mapping capture. For example, computational error in the mass balance of changes resulting from the added pumping (Equation 3) generally decreases with increasing pumping rate, Q_{well} . However, larger pumping rates increase the chances of the nonlinear responses described in the following paragraphs. Preliminary capture calculations can help in selecting a pumping rate that balances these problems. Preliminary capture calculations with pumpage at a few points near and far from features expected to be subject to capture can indicate ranges of transient capture responses. These can be used to select times for mapping capture.

Using MODFLOW as an example, calculations of capture outlined in the following sections can be made using any version of MODFLOW and the MODFLOW postprocessor Zonebudget (Harbaugh 1990). Features of interest can be represented using constant-head cells or one of the packages representing head-dependent boundaries. These include the river, drain, general-head boundary, stream, lake, and evapotranspiration packages. Most of these packages are documented in Harbaugh

(2005) and reports documenting previous versions of MODFLOW. The stream package used in the examples presented in this work is documented by Prudic (1989). The lake package is documented by Merritt and Konikow (2000). Needed flow terms are obtained from the volumetric mass balance in the listing file, cell-by-cell budget terms provided in files defined in the package input files, flows to and from groups of constant-head and head-dependent boundary cells as defined by the observation process (Hill et al. 2000; Harbaugh and Hill 2006), and zonal budgets produced by the postprocessor ZoneBudget.

Specified-flow (Neumann) boundary conditions in MODFLOW are simulated using, for example, the recharge package or well package. Flows to these boundaries are not affected by pumpage; therefore these features are not of interest in this work. Caution should be taken if the original model uses the multinode well (MNW) package (Halford and Hanson 2002; Konikow et al., 2009) because new wells may change conditions near the multinode wells and alter the distribution of pumping from the layers. When other groundwater flow models are used, similar capabilities generally are available and can be used to compute capture.

Practical Considerations for Constructing Capture Maps

Carrying out the steps outlined in the previous sections requires considerably more effort than making forward model runs. Care must be taken to get the best possible results for mapping using a reasonable amount of resources. The following sections outline some practical considerations for making repeated calculations of capture.

Nonlinearity

Examples in this paper express capture as a fraction of the added withdrawal rate. As was mentioned previously, if a system behaves linearly, capture fractions apply to other pumping rates. Also for a linear system, computed capture values could be used as response functions to determine combined effects of pumping at multiple locations. Nonlinearities are most likely to occur from changes in saturated thickness that significantly change transmissivity, as well as changes to the configuration of boundary conditions. For example, the nonlinearities of the MODLOW river, drain, and stream packages are described in McDonald and Harbaugh (1988; Figures 36, 41) and Prudic (1989; Figure 3). These changes can occur from the well being added to compute capture, or from other stresses being simulated. Kavetski and Kuczera (2007) suggest that many of the nonlinearities in models represent simplifications that may have been convenient to program but produce difficult situations in model analyses such as that considered in this work. Hill (2006) suggested that managing nonlinearity is an important part of building successful models.

Users of the methods outlined in this paper should consider testing the linearity of their models by computing and comparing capture fractions for different pumping

rates. For example, Leake et al. (2008b) show computed capture and rate of change in storage through time for two locations in the upper San Pedro model using withdrawal rates of 100 and 1000 m³/d. If a model exhibits highly nonlinear behavior, results of capture maps may only be valid for pumping rates close to the one used to construct the map. A map made for a particular pumping rate may nonetheless be useful in helping resource managers understand likely timing of capture. According to Leake et al. (2008b), the general effect of nonlinearity is to overestimate capture from groundwater pumping at higher pumping rates than the rate used to construct the capture map. Similarly, if attempts were made to linearize a model by keeping layer thickness (and therefore transmissivity) constant or removing nonlinearities in head-dependent boundaries, the effect would be to overestimate capture in areas where those nonlinearities are important in describing system behavior.

Additionally, in carrying out analyses of capture with a groundwater flow model, care should be taken that added pumping stresses do not change the configuration of specified flux boundaries. For example, addition of a new well can cause cells to go dry and turn off the original specified flux for the dry cells. The change in specified flux would produce a separate signal that could interfere with the estimate of capture. If this situation occurs, the options are to (1) use a lower withdrawal rate that does not cause cells to dry up or (2) ignore the calculation of capture for that location. As discussed by Bredehoeft et al. (1982), only the change in recharge induced by addition of a pumping well contributes to capture; the original recharge rate is irrelevant in the estimate of capture.

Automating Repeated Capture Calculations

Construction of a general purpose computer program to carry out steps needed for mapping capture would be possible. For examples shown here, however, custom programs were used. For the San Pedro, Deschutes, and synthetic examples (Figures 2, 3, and 5), FORTRAN programs were used. For the Kalamazoo example (Figure 4), Perl scripts were used. For each of these three examples, the program was customized for the particular model domain and model results being accessed to compute capture. These or other programming languages could be used for future analyses, as long as there is a way to repeatedly (1) construct a well package file for particular locations of interest, (2) run the model, (3) read budget results from appropriate output files, (4) make calculations of capture, and (5) save the results.

Features Simulated vs. Reality

Ideally, a model should include all head-dependent boundaries representing features from which capture can occur but should not include artificial or unrealistic head-dependent features and should not include unrealistic specified-flow boundaries that might affect computed capture at realistic head-dependent flow boundaries. Model boundaries that do not represent physical features in a way that they would respond to pumping stress

realistically are referred to here as “artificial model boundaries.” These boundaries typically are used to limit the represented model domain to an area smaller than the actual domain of the groundwater flow system. Artificial model boundaries may be specified-flow (including no-flow) and head-dependent flow boundaries. For example, no-flow boundaries have been used to terminate a model domain along a groundwater divide or along a groundwater flow line. Similarly, specified-head or head-dependent boundaries may be used to keep head in an area at a desired level and to possibly remove an area from the model in which head change is not expected. Artificial model boundaries are problematic in calculations of capture because they can affect calculation of capture from actual physical features represented with head-dependent boundaries. If artificial model boundaries exist, care must be taken to limit the extent of the capture map to locations where capture is almost entirely from head-dependent flow boundaries that represent physical features. For artificial head-dependent boundaries, some idea of how to limit the extent of the region to be mapped can be discerned by carrying out capture calculations for those boundaries. Where the value of $\Delta Q_{k,t}/Q_{\text{well}}$ for a transient model or $\Delta Q_{k,\infty}/Q_{\text{well}}$ for a steady state model is small, say less than 0.1, then effects of the nonphysical boundary (designated here by the subscript k) are minimal.

Similarly, if a model includes artificial specified-flow (including no-flow) boundary segments, mapped capture values may be erroneous. Care should be taken not to map capture values near these nonphysical boundaries.

Computation Time for Model Runs

Depending on the size of the region to be mapped, hundreds or even thousands of model runs may be required to construct a capture map. If possible, the model should be simplified to run efficiently for the period of time for which capture will be computed. Mapping capture does not necessarily require capture calculations for every grid cell. For examples presented in this paper, individual model run times typically were in the range of 1 to 3 min using a Windows® XP®-based computer with an Intel® Pentium® 3.0 GHz processor. The 1530 model runs needed to construct the San Pedro capture map (Figure 2) took slightly more than 2 d of computer time with serial execution of each forward run. These runs are independent and therefore are completely parallelizable.

Mass Balance in Computing Capture

When all potential features are included, the computed terms on the right side of Equation 3 should sum as closely as possible to 1.0. The difference between that value and 1.0 is the mass balance error in computing capture. These errors are numerical and indicate inadequate precision of model calculations caused by convergence criteria that are too large or possibly inadequate precision of the code. For example, a fully double precision version of MODFLOW may be needed, such as that posted on the web site for MODFLOW-2005. Because changes in storage and flow are divided by the

pumping rate of the added well, Q_{well} , numerical errors need to be small relative to Q_{well} . In computing capture maps using MODFLOW, experience has shown that mass balance errors in computing capture are highly correlated to the size of the flow rate listed as “IN-OUT” on the right-hand side of the volumetric mass balance (under “rates for this time step”) in the listing file. This value should be less than a few percent of Q_{well} . Larger errors result in a distorted or incorrect capture map, particularly if the mass balance error is related to computed changes in flow to or from features of interest, and not to the rate of change in storage.

Superposition

If an aquifer system responds linearly to withdrawals, capture maps can be made with groundwater superposition models (Cosgrove and Johnson 2005; Leake et al. 2008a). With this approach, the model uses an initial flat water surface and values of $Q_{1,t}$, $Q_{2,t}$, ..., $Q_{n,t}$, and $Q_{S,t}$ are zero. Change in pumping is simulated and quantities $\Delta Q_{1,t}$, $\Delta Q_{2,t}$, ..., $\Delta Q_{n,t}$, and $\Delta Q_{S,t}$ of Equations 2 and 3 are computed directly in budget calculations of the superposition model.

Results

Results from field studies include two transient maps of capture from all features and one transient capture map for one feature. These results show the utility of the capture fraction method in the analysis of complex systems. Finally, a synthetic example is used to show the steady state capture from one feature. The examples show the insights obtainable from these types of capture maps.

Two Field Examples of Transient Capture from All Features

Two examples of maps of transient capture from all head-dependent flow boundaries are used to show results from considering pumpage from anywhere within one hydrogeologic unit (represented here by a single model layer) of a three-dimensional model and pumpage from anywhere in an entire three-dimensional model.

The first map was made using a groundwater model of the Upper San Pedro Basin in southeastern Arizona, USA, and northern Sonora, Mexico (Figure 2; Pool and Dickinson 2007). The San Pedro River and associated riparian plants are in a narrow north-south trending band along the axis of the basin. Head-dependent boundaries in this area are simulated with MODFLOW-2000 and its stream, drain, and evapotranspiration packages. The model was converted from a series of temporally complex transient model runs that include seasonal pumping and other stresses. The simplified model was constructed by taking starting conditions from the steady state predevelopment model of Pool and Dickinson (2007) and keeping all specified-flow values constant from that model constant for a 100-year period, with the exception of the added pumping well used for computing capture. The 100-year period was simulated with 100 1-year time

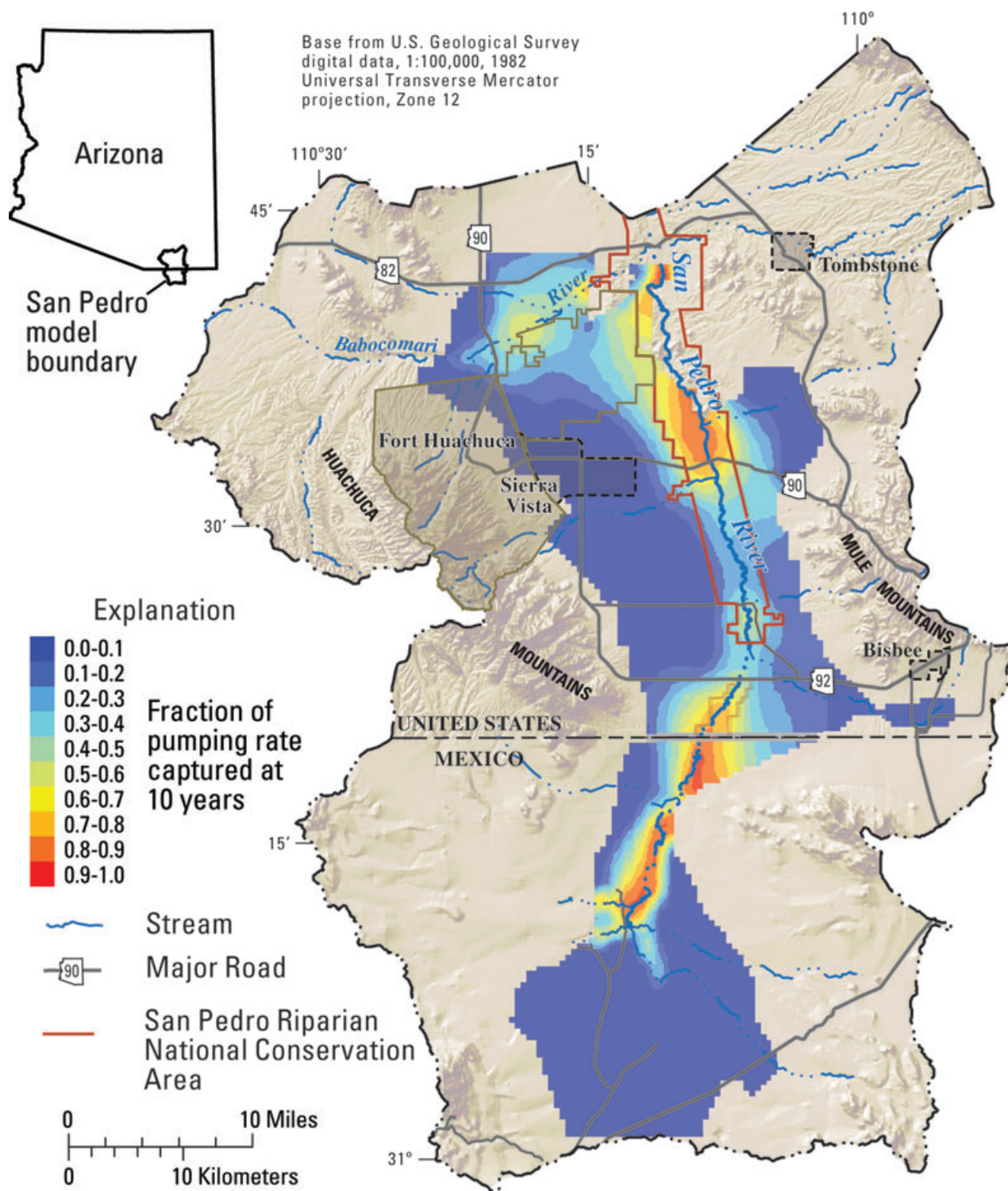


Figure 2. Computed capture of water from head-dependent boundaries as a function of well location in the Upper San Pedro Basin model layer corresponding to the lower basin fill for a pumping time of 10 years.

steps. Simulation of 100 years allows the opportunity to represent capture at a variety of times, animate the progression of capture through time (see link “Video showing simulated zones of capture of surface water by groundwater pumping, upper part of the San Pedro Basin,” at web site <http://az.water.usgs.gov>), or display capture curves through time for specific model locations (Leake

et al. 2008b; Figure 3). The grid spacing in the model is 250 m × 250 m. Pumping locations considered are at every fourth row and every fourth column, requiring 1530 model runs to compute capture values on a grid with a spacing of 1 km in both horizontal dimensions. There are five model layers. All pumping locations are in model layer 4, the layer corresponding to the lower basin fill

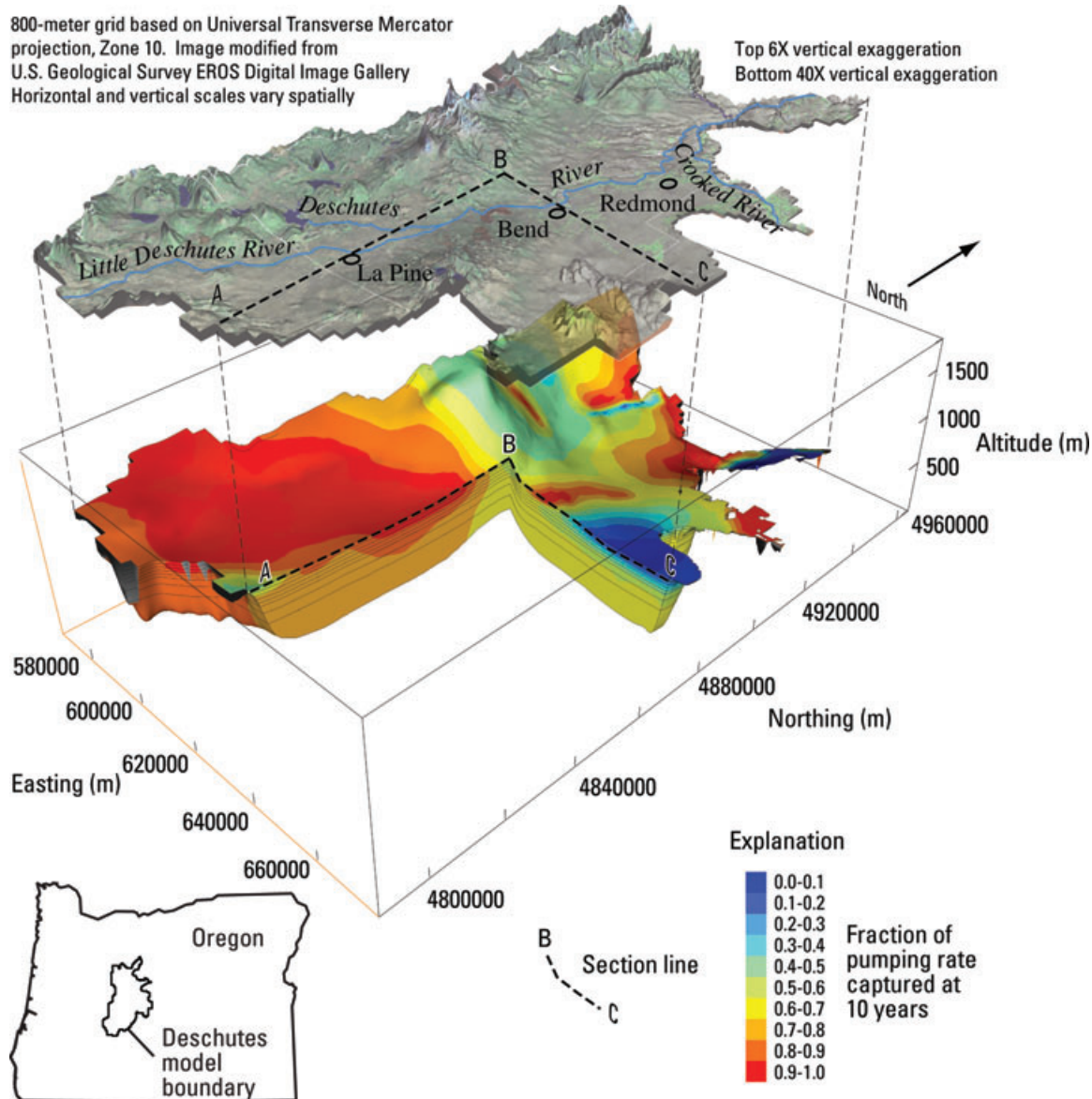


Figure 3. Cutaway view of representation of capture after pumping for 10 years in the upper Deschutes Basin, Oregon, model by Gannett and Lite (2004). Along section A–B, deep pumping would result in slower capture than shallow pumping but along section B–C, this pattern is reversed.

from which most wells in the area withdraw water. The example map of capture after 10 years of pumping is shown in Figure 2. Leake et al. (2008b) also show maps for capture from pumping at 50 years, and effects of enhanced flow to the river (the reverse of capture) from recharge to the uppermost saturated part of the aquifer for times for 10 and 50 years. With effects of pumping and recharge simulated for 100 years, maps could be created at any times of interest to resource managers up to 100 years. For the case of pumping, there is a general pattern of a higher fraction of capture near the river, but capture values vary somewhat along the river. The reason for the variation in timing of capture of water from the river and riparian system is that a silt and clay layer exists and is simulated between the pumped model layer 4 and the

riparian system in part of the area (Pool and Dickinson 2007).

The second example is a fully three-dimensional portrayal of transient capture from all head-dependent flow boundaries simulated using a model of the upper Deschutes Basin, Oregon (Figure 3; Gannett and Lite 2004). In this example, capture is calculated over the entire volume of the aquifer, allowing for analyses of differences in capture from both horizontal and vertical variations in pumping location. The Deschutes Basin model, constructed with MODFLOW-88, has an irregularly spaced finite-difference grid with 127 rows, 87 columns, and 8 layers of cells. The main boundaries from which capture can occur are the Deschutes River and tributaries and adjacent evapotranspiration areas. As for the San Pedro model, the Deschutes model

was modified to start with predevelopment steady state conditions and to simulate 100 years with 100 1-year time steps and constant stresses. Pumping locations considered included all of the active cells in the model domain, requiring 53,589 simulations. In this case, capture was only displayed at time of 10 years since the start of pumping. Simulation time could have been reduced by simulating less time than 100 years, with fewer than 100 time steps.

Results illuminate a number of important points about how hydrogeology represented in the model affects the timing of capture. For example, some hydrologists might assume that shallower pumping will result in more rapid capture than deeper pumping because head-dependent boundaries representing the river and evapotranspiration are at the top of the system. Results of capture at 10 years shown in the cutaway view (Figure 3) indicate that in the vicinity of section A–B, capture does indeed occur faster when pumping is shallow than when pumping is from further down in the system. However, in the vicinity of section B–C, vertical leakance between layers is low, causing drawdown from pumping at depth to propagate more quickly laterally to reach distant head-dependent boundaries. In contrast, shallow pumping near section B–C allows greater access to the larger storage capacity provided by the specific yield of the top layer, thereby slowing the propagation of drawdown toward distant head-dependent boundaries.

One Field Example of Transient Capture from One Feature

An example capture map showing transient capture from one feature was generated using the MODFLOW-based groundwater flow model developed for Kalamazoo County, Michigan (Luukkonen et al. 2004). This model has 6 layers, 154 rows, and 162 columns, and the grid spacing in the area of interest is 200 m × 200 m. The 5-year transient simulation includes pumping and recharge that varies seasonally that was retained for this example. The only change to the model was that the river package part of the observation process within MODFLOW was used to simulate the flux to individual segments of a stream network. Potential capture from the stream segment of interest by a well in the watershed of that segment is shown (Figure 4). This capture map was generated using well locations in every other row and column in layer 3 of the model within the watershed of interest, omitting cells containing the river package for the segment considered. The capture analysis required 208 model runs. At 5 years, capture from a stream is shown to vary from less than 0.1 to approximately 0.8 of the pumping rate. Capture at 5 years lessens with distance from the stream segment because of ongoing storage change, as well as possible capture from head-dependent boundaries in adjacent watersheds. Results within the watershed of interest, which is part of a much larger area simulated, therefore are affected by boundaries other than the feature of interest.

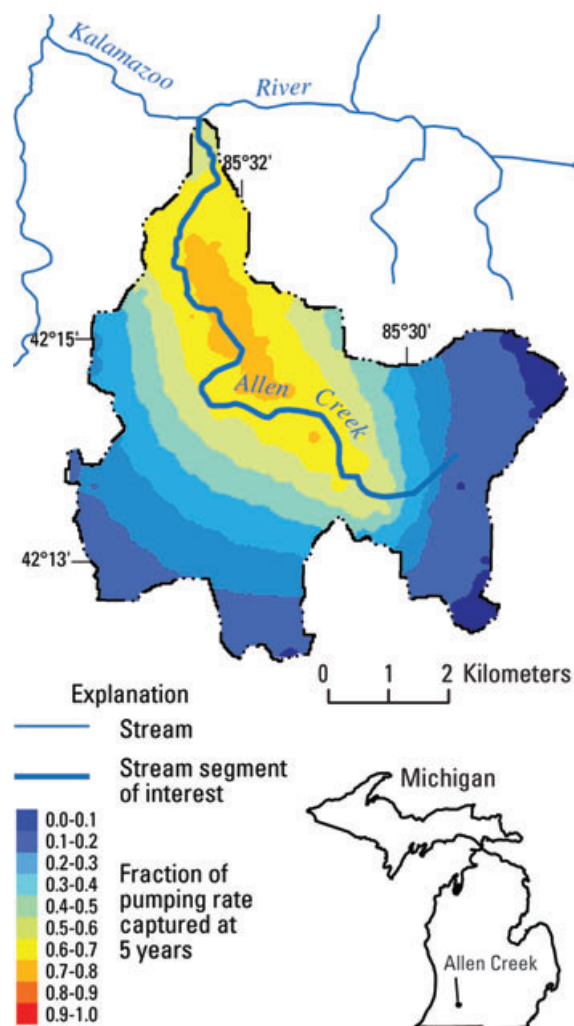


Figure 4. Example capture map showing fraction of pumping after 5 years supplied by a selected river segment in the Kalamazoo region groundwater flow model (Luukkonen et al. 2004).

One Synthetic Example of Ultimate Steady State Capture from One Feature

A synthetic model for a steady state capture map was adapted from a sample problem in Hill and Tiedeman (2007; Figure 2.1). The model has 18 rows and 18 columns with an equal horizontal grid spacing of 1000 m (Figure 5A). Upper and lower aquifers, each 50 m thick, are simulated with two model layers. An intermediate 10-m thick confining layer is simulated without use of a separate model layer. Nonuniform specified recharge occurs in the upper layer, and a river is in column 1 of the upper layer on the west side of the model domain. For this example, the river has been divided into three reaches of equal length as shown in Figure 5A. Along the east side of the model in column 18, a general-head boundary simulates subsurface connection to an adjoining hillside. The bed conductance of the general-head boundary, however, is so low that its presence does not affect capture calculations. For more information on the model setup and parameters, see Hill and Tiedeman (2007).

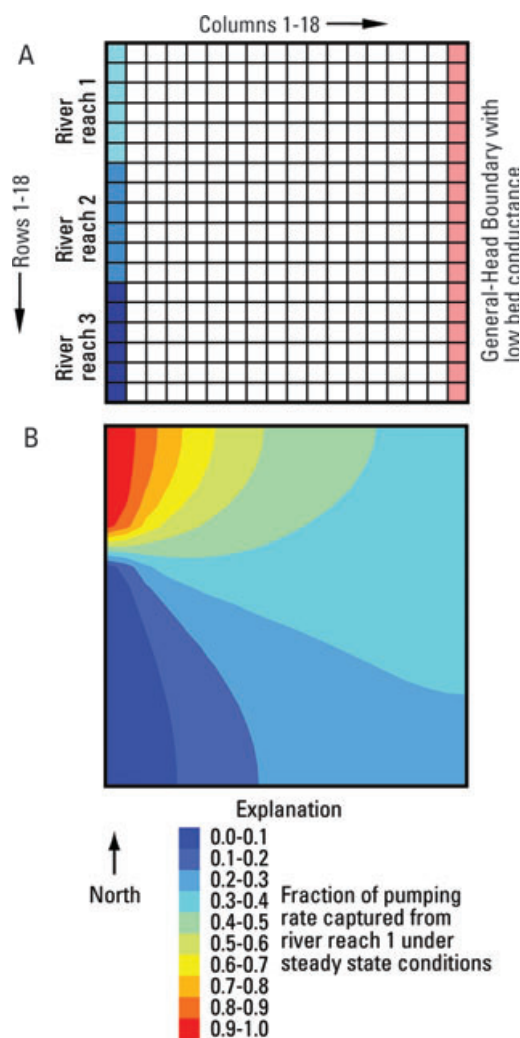


Figure 5. Example steady state capture map showing (A) model setup and (B) capture fraction from reach 1 as a function of pumping location in layer 1.

Mapped results of capture from reach 1 by pumping in layer 1 show that, as expected, capture is high for pumping locations near reach 1, is low for locations near reaches 2 and 3, and is intermediate for reaches to the east in which capture occurs more equally from the three reaches (Figure 5B). The nonuniform specified recharge distribution has no effect on the capture map, but if complex spatial distributions of hydraulic conductivity were introduced, shapes of the zones would be different. Similarly, if the conductance of the general-head boundary in column 18 had been high enough to allow significant capture from that feature, the computed capture zones would have been different.

Discussion

Applicability and Limitations

Capture maps are best used to help understand the relation between location of pumping and the timing of capture. They can help the modeler understand how hydrogeologic features such as clay layers or properties

such as vertical anisotropy (the ratio of horizontal to vertical hydraulic conductivity) affect the location and timing of capture. Maps are made using hundreds or even thousands of model runs over a significant area represented in a groundwater model. Results shown, however, do not mean that pumping at a rate of interest from a given location is logistically, politically, or technically possible or feasible. For site-specific studies, regional capture maps can be used as a first assessment of locations at which the model-predicted capture rate is in an acceptable range. That step should be followed up with more site-specific model investigations when wells are pumped at specific locations of interest.

Beyond Capture Maps

As was mentioned previously, capture fractions are a type of aquifer response function used in management optimization models. If capture fractions are saved for different pumping times for a reasonably linear model, values can be used to compute capture for various complex scenarios without additional runs of the model. For example, capture fractions could be used with convolution to compute capture from a well with a time-varying pumping rate. A similar process could be used to compute combined capture from multiple wells at different locations. The fractions could also be used to calculate response to recharge instead of pumping.

Conclusions

The capture fraction maps presented here can be used to help water managers and the general public understand how the position of a well and time since pumping began can affect capture of water from rivers, springs, streams, and wetlands. Hydrologists generally make graphs of capture vs. time for select points of interest. Mapping capture over an area or region for a time of interest involves making many model runs, each time with a well in a different location. The process can be automated with a computer program. Types of capture maps include transient capture from all head-dependent flow boundaries, transient capture from a particular head-dependent flow boundary, and ultimate steady state capture from a particular head-dependent flow boundary. Care should be taken to assure that the mass balance in computing capture is as close to zero as possible.

Acknowledgments

This work was supported by the National Water Availability and Use Pilot Program of the U.S. Geological Survey. Comments from reviewers Mary Chapiga, Carol Luukkonen, and Mary Hill of the U.S. Geological Survey and two anonymous reviewers greatly improved the manuscript. The authors thank Don Pool, Marshall Gannett, and Carol Luukkonen of the U.S. Geological Survey for making their models available to us for development and testing of the capture fraction method.

References

- Barlow, P.M., and D.C. Dickerman. 2001. Numerical-simulation and conjunctive-management models of the Hunt-Annaquatucket-Pettaquamscutt stream-aquifer system, Rhode Island. U.S. Geological Survey Professional Paper 1636. Reston, Virginia: USGS.
- Bredehoeft, J.D., S.S. Papadopoulos, and H.H. Cooper Jr. 1982. Groundwater: The water budget myth. In *Scientific Basis of Water-Resources Management*, ed. National Research Council (U.S.), Geophysical Study Committee, 51–57. Washington, D.C.: National Academy Press.
- Burns, A.W. 1983. Simulated hydrologic effects of possible groundwater and surface water management alternatives in and near the Platte River, south-central Nebraska. U.S. Geological Survey Professional Paper 1277-G. Reston, Virginia: USGS.
- COHYST Technical Committee. 2004. The 40-year, 28-percent stream depletion lines for the COHYST area west of Elm Creek, Nebraska. http://cohyst.dnr.ne.gov/adobe/dc012_28-40_lines_092104.pdf (accessed August 4, 2009).
- Cosgrove, D.M., and G.S. Johnson. 2005. Aquifer management zones based on simulated surface-water response functions. *Journal of Water Resources Planning and Management* 131, no. 2: 89–100.
- Cosgrove, D.M., and G.S. Johnson. 2004. Transient response functions for conjunctive water management in the Snake River Plain, Idaho. *Journal of the American Water Resources Association* 40, no. 6: 1469–1482.
- Gannett, M.W., and K.E. Lite Jr. 2004. Simulation of regional ground-water flow in the upper Deschutes Basin, Oregon. U.S. Geological Survey Water-Resources Investigations Report 03–4195. Reston, Virginia: USGS.
- Glover, R.E., and G.G. Balmer. 1954. River depletion resulting from pumping a well near a river. *Transactions of the American Geophysical Union* 35, no. 3: 468–470.
- Halford, K.J., and R.T. Hanson. 2002. User guide for the drawdown- limited, multi-node well (MNW) package for the U.S. Geological Survey's modular three-dimensional finite-difference ground-water flow model, versions MODFLOW-96 and MODFLOW-2000. U.S. Geological Survey Open-File Report 02-293. Reston, Virginia: USGS.
- Harbaugh, A.W. 2005. MODFLOW-2005. The U.S. Geological Survey modular ground-water model—The ground-water flow process. U.S. Geological Survey Techniques and Methods 6-A16. Reston, Virginia: USGS.
- Harbaugh, A.W. 1990. A computer program for calculating subregional water budgets using results from the U.S. Geological Survey modular three-dimensional ground-water flow model. U.S. Geological Survey Open-File Report 90-392. Reston, Virginia: USGS.
- Harbaugh, A.W., and M.C. Hill. 2006. Observation process of MODFLOW-2005. Unpublished document obs.pdf. <http://water.usgs.gov/nrp/gwsoftware/modflow2005/OBS.pdf> (accessed August 18, 2009).
- Harbaugh, A.W., E.R. Banta, M.C. Hill, and M.G. McDonald. 2000. MODFLOW-2000, The U.S. Geological Survey modular ground-water model—User guide to modularization concepts and the ground-water flow process. U.S. Geological Survey Open-File Report 00-0092. Reston, Virginia: USGS.
- Hill, M.C. 2006. The practical use of simplicity in developing ground water models. *Ground Water* 44, no. 6: 775–781.
- Hill, M.C., and C.R. Tiedeman. 2007. *Effective Groundwater Model Calibration*. New Jersey: John A. Wiley & Sons.
- Hill, M.C., E.R. Banta, A.W. Harbaugh, and E.R. Anderson. 2000. MODFLOW-2000, the U.S. Geological Survey modular ground-water model—User guide to the observation, sensitivity, and parameter-estimation processes and three post-processing programs. U.S. Geological Survey Open-File Report 00–184. Reston, Virginia: USGS.
- Jenkins, C.T., and O.J. Taylor. 1974. A special planning technique for stream-aquifer systems. U.S. Geological Survey Open-File Report 74-242. Reston, Virginia: USGS.
- Kavetski, D., and G. Kuczera. 2007. Model smoothing strategies to remove microscale discontinuities and spurious secondary optima in objective functions in hydrological calibration. *Water Resource Research* 43: W03411.
- Konikow, L.F., G.Z. Hornberger, K.J. Halford, and R.T. Hanson. 2009. Revised multi-node well (MNW2) package for MODFLOW ground-water flow model. U.S. Geological Survey Techniques and Methods 6-A30. Reston, Virginia: USGS.
- Leake, S.A., W. Greer, D. Watt, and P. Weghorst. 2008a. Use of superposition models to simulate possible depletion of Colorado River water by ground-water withdrawal. U.S. Geological Survey Scientific Investigations Report 2008–5189. Reston, Virginia: USGS.
- Leake, S.A., D.R. Pool, and J.M. Leenhouts. 2008b. Simulated effects of ground-water withdrawals and artificial recharge on discharge to streams, springs, and riparian vegetation in the Sierra Vista subwatershed of the Upper San Pedro Basin, southeastern Arizona. U.S. Geological Survey Scientific Investigations Report 2008–5207. Reston, Virginia: USGS.
- Leake, S.A., J.P. Hoffmann, and J.E. Dickinson. 2005. Numerical ground-water change model of the C aquifer and effects of ground-water withdrawals on stream depletion in selected reaches of Clear Creek, Chevelon Creek, and the Little Colorado River, northeastern Arizona. U.S. Geological Survey Scientific Investigations Report 2005–5277. Reston, Virginia: USGS.
- Luukkonen, C.L., S.P. Blumer, T.L. Weaver, and J. Jean. 2004. Simulation of the ground-water-flow system in the Kalamazoo County area, Michigan. U.S. Geological Survey Scientific Investigations Report 2004–5054. Reston, Virginia: USGS.
- Maddock, T.M. III, and L. Lacher. 1991. Drawdown, velocity, storage, and capture response functions for multiaquifer systems. *Water Resource Research* 27, no. 11: 2885–2898.
- McDonald, M.G., and A.W. Harbaugh. 1988. A modular three-dimensional finite-difference ground-water flow model. U.S. Geological Survey, Techniques of Water-Resources Investigations, 6-A1. Reston, Virginia: USGS.
- Merritt, L.M., and L.F. Konikow. 2000. Documentation of a computer program to simulate lake-aquifer interaction using the MODFLOW ground-water flow model and the MOC3D solute-transport model. U.S. Geological Survey Water-Resources Investigations Report 00-4167. Reston, Virginia: USGS.
- Peterson, S.M., J.S. Stanton, A.T. Saunders, and J.R. Bradley. 2008. Simulation of ground-water flow and effects of ground-water irrigation on base flow in the Elkhorn and Loup River Basins, Nebraska. U.S. Geological Survey Scientific Investigations Report 2008–5143. Reston, Virginia: USGS.
- Pool, D.R., and J.E. Dickinson. 2007. Ground-water flow model of the Sierra Vista subwatershed and Sonoran portions of the Upper San Pedro Basin, southeastern Arizona, United States, and northern Sonora, Mexico. U.S. Geological Survey Scientific Investigations Report 2006–5228. Reston, Virginia: USGS.
- Prudic, D.E. 1989. Documentation of a computer program to simulate stream-aquifer relations using a modular, finite-difference, ground-water flow model. U.S. Geological Survey Open-File Report 88–729. Reston, Virginia: USGS.
- Theis, C.V. 1940. The source of water derived from wells: Essential factors controlling the response of an aquifer to development. *Civil Engineer* 10: 277–280.